Environmental Science and Pollution Research (2022) 29:768–778
https://doi.org/10.1007/s11356-021-15688-3

RESEARCH ARTICLE

Simultaneous removal of heavy metals and bioelectricity generation in microbial fuel cell coupled with constructed wetland: an optimization study on substrate and plant types

Lu Wang[1] · Dayong Xu[1] · Qingyun Zhang[1] · Tingting Liu[1] · Zhengkai Tao[1]

Received: 5 May 2021 / Accepted: 23 July 2021 / Published online: 2 August 2021

Abstract

A microbial fuel cell coupled with constructed wetland (CW-MFC) was built to remove heavy metals (Zn and Ni) from sludge. The performance for the effects of substrates (granular activated carbon (GAC), ceramsite) and plants (*Iris pseudacorus*, *water hyacinth*) towards the heavy metal treatment as well as electricity generation was systematically investigated to determine the optimal constructions of CW-MFCs. The CW-MFC systems possessed higher Zn and Ni removal efficiencies as compared to CW. The maximal removal rates of Zn (76.88%) and Ni (66.02%) were obtained in system CW-MFC based on GAC and *water hyacinth* (GAC- and WH-CW-MFC). Correspondingly, the system produced the maximum voltage of 534.30 mV and power density of 70.86 $mW{\cdot}m^{-3}$, respectively. Plant roots and electrodes contributed supremely to the removal of heavy metals, especially for GAC- and WH-CW-MFC systems. The coincident enrichment rates of Zn and Ni reached 21.10% and 26.04% for plant roots and 14.48% and 16.50% for electrodes, respectively. A majority of the heavy metals on the sludge surface were confirmed as Zn and Ni. Furthermore, the high-valence Zn and Ni were effectively reduced to low-valence or elemental metals. This study provides a theoretical guidance for the optimal construction of CW-MFC and the resource utilization of sludge containing heavy metals.

Keywords CW-MFC · Heavy metal · Sludge · Bioelectricity · Substrate and plant types

Introduction

Biotechnology, as an efficient sewage treatment method, has been widely applied to the municipal sewage plant. However, these biological processes are reported to form large amounts of excess sludge with complicated ingredients (Ke et al. 2012). As a result, the handling and disposal of sludge require a lot of financial and material capabilities of municipal sewage plant (Qian et al. 2016). It is therefore imperative to develop affordable and effective technologies to enable a sufficient disposal of sludge. Several strategies, including bioleaching (Chen and Cheng 2019), chemical extraction (Liu et al. 2018c), electrokinetics (Gao et al. 2013), and hydrothermal carbonization (Liu et al. 2018b), emerged for heavy metal removals or pathogen disinfection from sludge. The chemical utilization or complex operation of these techniques gave rise to the limitation for effective sludge treatment (Hu et al. 2021). Due to its high chemical energy, a sustainable development proposal was also put forward by utilizing sludge as renewable energy source to the land (Zhou et al. 2020). Nevertheless, the accumulation of heavy metals in the sludge generated by wastewater treatment processes caused potential risks to animals and humans through the food chain, thereby limiting the application of sludge (Shamsollahi et al. 2019; Yang et al. 2013). Therefore, the development of cost-effective and energy-neutral technologies is currently the most desired approach (Gupta et al. 2021).

Responsible Editor: Alexandros Stefanakis

Highlights a. Six lab-scaled CW-MFCs were constructed to remove Zn and Ni from sludge.
b. GAC and *water hyacinth* boosted the heavy metal removal and bio-electricity generation.
c. High-valence Zn and Ni were effectively reduced to low-valence or elemental metals.
d. The findings may be extended to the treatment of refractory heavy metals from excess sludge.

✉ Qingyun Zhang
zhangqingyun@ahpu.edu.cn

[1] School of Chemical and Environmental Engineering, Anhui Polytechnic University, Wuhu 241000, Anhui, China

Constructed wetlands (CWs) were designed to simulate the natural purification of pollutants by the wetland plants, substrates, and microorganisms (Shen et al. 2018). CWs displayed potential applicability for the treatment of sludge containing heavy metals because of its simple technological process, low operation cost, and good purification capacity (Fan et al. 2013; Zhong et al. 2020). For instance, a sludge treatment wetland with ventilation was conducted by a scholar to analyze the removal and fate of heavy metals from excess sludge (Meng et al. 2020). However, the anaerobic conditions in the lower sections of CWs resulted in the slow decomposition of organic matters and lack of favorable electron acceptors (Srivastava et al. 2017). As a consequence, high concentration of sludge organics was not only underutilized in CW process, but also increased its operating load.

Microbial fuel cell (MFC), as a promising purification technology, has been applied to boost the performance for the removal of heavy metals (Xu et al. 2019). Of Cr(VI), 80 mg·L^{-1} was reported to be completely removed within 72 h and bio-electrochemically reduced to nontoxic Cr(III) in a dual-chamber MFC (Li et al. 2018). The device MFCs required anode (anaerobic) and cathode (aerobic) regions, which were highly matched with CWs (Xu et al. 2021). On this basis, an integrated CW-MFC biotechnology was of great significance for enhancing the wastewater treatment containing heavy metals (Xu et al. 2019; Zhong et al. 2020). A removal study of Pb(II) by CW-MFC displayed that the removal rate was up to 85% with a maximum power density of 7.432 mW·m^{-3} (Zhao et al. 2020). In another study, approximately 91% removal of Cr(VI) was obtained in CW-MFC under the optimal operating conditions (Mu et al. 2020).

Substrate and plant types were considered as important parameters for optimizing CW-MFCs (Di et al. 2020; Ge et al. 2020). The addition of optimal substrate to the CW-MFCs had been reported to enhance strongly the treatment of pollutants and prolong the running period (Wang et al. 2020). Plant roots were capable of removing pollutants directly from wastewater by adsorption and enrichment (Zhou et al. 2018). Meanwhile, root exudates could provide carbon and energy source for the growth of rhizosphere microorganisms (Wang et al. 2017). However, detailed information about the heavy metal removal from sludge by CW-MFCs, based on optimized substrate and plant types, is still scarce.

Herein, six lab-scaled CW-MFCs were constructed to investigate the performance of substrate and plant types on the removal of heavy metals (Zn and Ni), so as to determine the optimal construction. The power generation and other electrochemical indices were determined by a paperless recorder (MIK-9600). XRD analysis was used to characterize the migration and transformation of Zn and Ni in CW-MFCs. The findings in this study will provide guidance for the optimal construction of CW-MFC and the resource utilization of sludge containing heavy metals.

Materials and methods

CW-MFC construction and untreated sludge

Vertical lab-scaled CW-MFC systems were built as polyacrylic plastic columns with an inner diameter of 15 cm and a height of 40 cm (Fig. 1). From the bottom upward, the device was filled up as follows: a support layer, an anode layer, a separation layer, and a sludge layer. Carbon clothes incorporating stainless steel meshes were embedded into the anode and sludge layer to serve as the anode and cathode (12 cm apart), respectively. The external circuit was connected to the 1000-Ω resistance by the copper wire. The untreated sludge was the mixture in 1:1 (v/v) ratio of the anaerobic and industrial sludge collected from sewage treatment plant and automobile enterprise in Wuhu, Anhui, China. Detailed CW-MFC construction and the properties of the untreated sludge were described previously (Liu et al. 2020).

Experimental operation

Granular activated carbon (GAC) and ceramsite (3–5 mm in diameter, respectively) were selected as fillers for the anode layer to evaluate the effect of substrate types on the performance of CW-MFC. Additionally, the emergent plant *Iris pseudacorus* and floating plant *water hyacinth* were irrigated with tap water for 1 week and then transplanted into the sludge layer to remove the heavy metals. For the purpose of this work, six CW-MFC devices were prepared and divided into two groups in this experiment. CW, the traditional constructed wetland, was set as the blank control filled with GAC. NP-CW-MFC was built with GAC in the anode layer but without any plant materials. GAC- and CER-CW-MFC were, respectively, filled with granular activated carbon and ceramsite in the anode layer and planted with *water hyacinth* in the sludge layer. Plant materials (*Iris pseudacorus* and *water hyacinth*) were, respectively, transplanted into the CW-MFC system to prepare the IP- and WH-CW-MFC systems.

At the start-up period, the anaerobic sludge collected from sedimentation tank of Zhujiaqiao Wastewater Treatment Plant (Wuhu, Anhui, China) was mixed with nutrient solution in 1:1 (v/v) ratio and subsequently inoculated into the CW-MFCs (Wang et al. 2019). The nutrient solution consisted of (L^{-1}) $C_6H_{12}O_6$ 0.4717 g, KH_2PO_4 0.9 g, $K_2HPO_4{\cdot}3H_2O$ 0.68 g, NH_4Cl 0.1 g, $CaCl_2$ 0.1 g, EDTA 0.1 g, $MgCl_2{\cdot}6H_2O$ 0.1 g, $MnSO_4{\cdot}H_2O$ 0.2 mg, $CoCl_2{\cdot}6H_2O$ 2.4 mg, $CuCl_2{\cdot}2H_2O$ 1 mg, $FeCl_2$ 1 mg, and $ZnCl_2$ 5 mg. After a 2-week adaptation period, the untreated sludge was added into the CW-MFC systems. The COD of anode liquor was monitored at regular intervals and kept around 500 mg/L by the addition of glucose. Anolyte and sludge samples were collected in triplicate every 4 days.

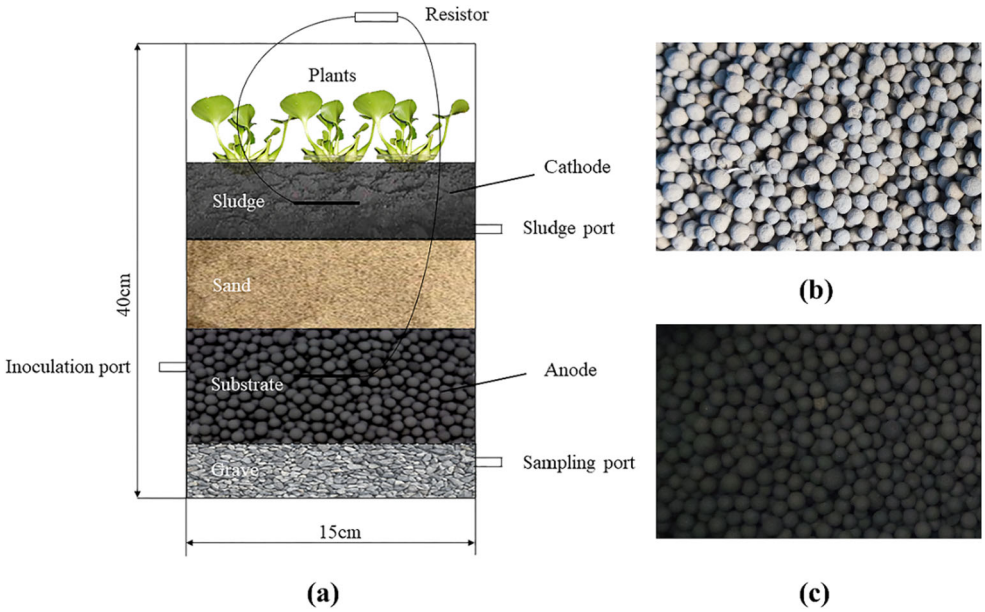

Fig. 1 Diagrams of vertical lab-scaled CW-MFC (**a**) as well as the ceramsite (**b**) and GAC (**c**) used in CW-MFC (Liu et al. 2020)

The concentration of heavy metals as well as physiochemical indexes, including pH and oxidation-reduction potential (ORP), was tested immediately after sampling. Finally, the plant and electrode were sampled for heavy metal determination. All the CW-MFCs were exposed to a natural environment simulated by setting 12-h light-dark cycles on 80-W LED lights at a room temperature of 20–30°C.

Analytical methodology

Determination and valence analysis of heavy metals

Sludge and plant (roots, stems, and leaves) samples were dried at 105°C for 24 h and then were ground into powder. Digested were 0.2 g and 0.15 g of sieved sludge and plant, respectively, with 10-mL aqua regia (HNO_3·3HCl), 5-mL $HClO_4$, and 2-mL concentrated H_2SO_4 in a PTFE tube for 24 h. Then the digestion tubes were, respectively, heated at 185°C for 3 h and 205°C for 7 h by the COD rapid digestion apparatus (SN-102A, Sunde Environmental Protection Technology Ltd., China). The cooled digestion solution was passed through the filter membrane (0.45 μm) to eliminate impurities and then diluted to 50 mL. The sludge leachate and aqua regia soaked with electrodes also underwent such filtration and constant volume operation. Finally, the concentrations of heavy metals in digested sludge and plant samples, as well as in sludge leachate and soaking solution, were determined by a flame atomic absorption spectrometer (TAS-990, Purkinje General Instrument Ltd., China) (Liu et al. 2020). The chemical forms of the elements on the surface of sludge were characterized by X-ray photoelectron spectroscopy (XPS, AXIS NOVA, Shimadzu, Japan).

Water quality determination

COD was tested by the fast digestion spectrophotometric method (HJ/T399-2007). The pH and ORP were measured using a portable pH/ORP meter (PHB-4, Shanghai Leici).

Measurement of electrical performance

The voltage date across the external resistor was collected by a paperless recorder (MIK-9600). The current density (I, mA/m^{-3}) and power density (P, mW/m^{-3}) were calculated according to the equations $I = \frac{U}{RV}$ and $P = \frac{U^2}{RV}$, where U, R, and V indicate the voltage (V), electric resistance (Ω), and effective working volume of anode (m^3), respectively. When the bioelectrogenesis entered the stable period, the power density and polarization curves were measured by varying the external resistance over a range of 100–10,000 Ω to acquire the corresponding voltage. Then the curves were obtained by plotting the voltage or power density versus current density.

Data analysis

In this study, the removal rate was calculated, and the curves in the figures were plotted in Origin 8.5 from the mean values of 6 batches. In addition, XPS Peak 4.1 software was used for valence analysis of heavy metals.

Results and discussion

Effect of substrate and plant types on pH and ORP

The pH values of anode solution in CW-MFC systems ranged from 6.70 to 7.08 (Table 1), indicating that CW-MFCs possessed better performance in microneutral environment. It was noted that the CW-MFCs filled with GAC presented a weak acidity (<7.0). Hence, CW-MFCs played a similar role in regulating the pH of anode area in comparison with CW reactor, especially for systems based on GAC.

ORP reflected the macroscopic oxidation-reduction behavior of all substances in aqueous solution. It was considered as the crucial parameter to monitor the anode anaerobism and cathode aerobism, which affected the pollutant removal and energy recovery in the CW-MFC (Doherty et al. 2015). According to Table 1, the redox gradient of anode and cathode was arranged as follows: GAC-CW-MFC>WH-CW-MFC>CER-CW-MFC>IP-CW-MFC>CW>NP-CW-MFC. Therefore, GAC had more advantages over ceramsite to maintain a higher redox gradient. The presence of plants exhibited a positive effect on the redox gradient of CW-MFC, which was consistent with the previous report (Teoh et al. 2020). This was mainly a result of the increased surface availability of the microorganism biofilm and the release of oxygen to the rhizosphere through photosynthesis by the wetland plants (Di et al. 2020). Notably, *water hyacinth* was superior to *Iris pseudacorus* in enhancing the redox gradient. It might be that the immoderate elongation caused by *Iris pseudacorus* roots destroyed the anaerobic environment and resulted in the high anode ORP (Liu et al. 2014).

Bioelectricity generation of CW-MFCs

Output voltage

The real-time output voltage and the maximum voltage of CW-MFC systems operated in the closed-circuit mode were monitored during the experiment period. As evident in Fig. 2, the output voltage of each system presented an obvious cyclical trend from increase to decrease during the first 40 days with the injection of nutrient solution. This might be attributed to the increased nutrient requirements of the electricigens caused by the nutrient solution, which was conducive to the system productivity. When the experiment entered the later period, the output voltage was basically stable due to the stability of CW-MFC systems.

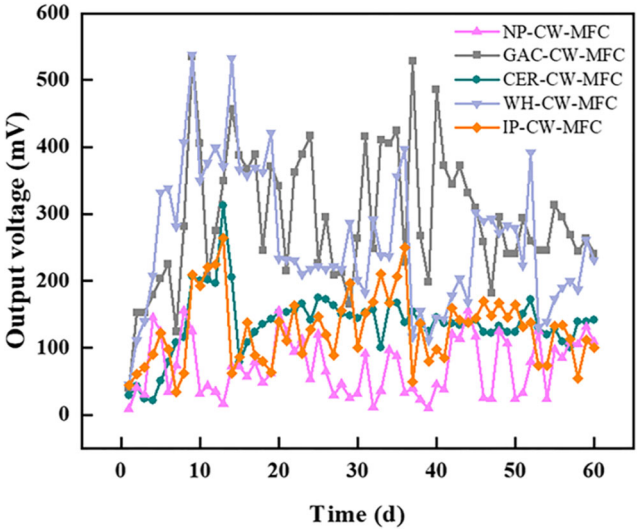

Fig. 2 Output voltages of different CW-MFC systems

GAC-CW-MFC produced a maximum voltage of 534.30 mV, which was about 70.62% higher than that of assay CER-CW-MFC (Table 2). Ceramsite had been reported to inhibit the growth of electrochemically active bacteria as a result of its high iron content and low available surface area (Xu et al. 2021; Zhong et al. 2020). Furthermore, the microorganisms grown in the ceramsite converted a mass of substrate into methane instead of electrons, which contributed greatly to the low electricity generation performance (Liu et al. 2014; Zhang et al. 2020). In contrast, the high conductivity of GAC made it more conducive to electron transfer, thereby exhibiting better electrical properties. Therefore, GAC might be more suitable for the growth of exoelectrogens in comparison to the ceramsite. The maximum voltages of NP-CW-MFC, WH-CW-MFC, and IP-CW-MFC were 155.40, 537.64, and 250.52 mV, respectively. Obviously, the presence of plants, especially for *water*

Table 1 pH and ORP of different CW-MFC systems

Parameters	CW	NP-CW-MFC	GAC-CW-MFC	CER-CW-MFC	WH-CW-MFC	IP-CW-MFC
Anode pH	6.88	6.84	6.70	7.08	6.92	6.83
Anode ORP (mV)	−125	−132	−254	−221	−205	−152
Cathode ORP (mV)	102	93	128	105	151	143
ORP gradient (mV)	227	225	382	326	356	295

Note: CW, traditional constructed wetland; NP-CW-MFC, CW-MFC without any plant materials; GAC-CW-MFC, CW-MFC filled with granular activated carbon in the anode layer; CER-CW-MFC, CW-MFC filled with ceramsite in the anode layer; WH-CW-MFC, CW-MFC planted with *water hyacinth* in the sludge layer; IP-CW-MFC, CW-MFC planted with *Iris pseudacorus* in the sludge layer

Table 2 The power generation performance of different CW-MFC systems

Systems	Maximum voltage (mV)	Internal resistance (Ω)	Maximal power density ($mW·m^{-3}$)
NP-CW-MFC	155.40	683.58	0.86
GAC-CW-MFC	534.30	587.98	70.86
CER-CW-MFC	313.21	787.90	16.66
WH-CW-MFC	537.64	533.85	27.91
IP-CW-MFC	250.52	583.43	9.88

hyacinth, was conductive to boosting the power generation. This might be attributed to the oxygen excreted by plant roots as a viable alternative source of electron acceptors for CW-MFC (Chen et al. 2012; Villasenor et al. 2013). Besides, the plant roots could alleviate the blockage caused by the rapid growth of biofilm, which was beneficial to the diffusion of protons produced by electrochemically active bacteria (Wang et al. 2017). A CW-MFC study of *Iris pseudacorus* was reported to penetrate the roots into the anode to release oxygen, resulting in the co-existence of aerobic bacteria to compete with electroactive bacteria for the utilization of organic matter and then further reduce bioelectricity production (Liu et al. 2018a). Thus, it might be speculated that the root effect of *water hyacinth* in CW-MFC could provide more organic matter for the growth of electrochemically active bacteria as compared to *Iris pseudacorus*. In summary, GAC and *water hyacinth* were, respectively, the optimal substrate and plant for the CW-MFC output voltage.

Polarization curves and internal resistance analysis

During the stable operation period, the power density and polarization curves of CW-MFCs were measured (Fig. 3). The results indicated that the power output differed markedly by the addition of substrates and plants among the five systems. Especially, the systems NP-CW-MFC, GAC-CW-MFC, CER-CW-MFC, WH-CW-MFC, and IP-CW-MFC reached the maximal power densities of 0.86, 70.86, 16.66, 27.91, and 9.88 $mW·m^{-3}$, respectively (Table 2). Polarization curves provided valuable information about the activation, ohmic, and concentration losses which adversely affect the electrogenesis capacity of MFC (Logan et al. 2006; Srivastava et al. 2015). In this experiment, the polarization curve of CW-MFC with approximate linearity was mainly the ohmic polarization region. The output voltage and polarization curve decreased linearly with the increase of current density. As a consequence, the apparent internal resistance of MFCs could be calculated according to the slope of the polarization curve (Table 2).

The system CER-CW-MFC had the highest internal resistance (787.9 Ω), followed by NP-CW-MFC (683.58 Ω), GAC-CW-MFC (587.98 Ω), IP-CW-MFC (583.43 Ω), and WH-CW-MFC (533.85 Ω). Thus, ceramsite employed as the substrate strongly enhanced the system internal resistance. On the contrary, the cultivation of plants played an important role in reducing the internal resistance. This effect was attributed to the fact that plants could increase the number of cathode microorganisms and accelerate the oxygen reduction reaction, thereby reducing the internal resistance (Fang et al. 2013). Little difference in internal resistance of systems WH-CW-MFC and IP-CW-MFC was noted, whereas the maximum voltage and power density varied remarkably. This might be related to the differences of redox gradient caused by oxygen transfer and anaerobic environment destruction in the roots of two wetland plants (Liu et al. 2014). In conclusion, the root depth and distribution of wetland plants were imperative to be considered to avoid the breakdown of CW-MFC system (Helder et al. 2010).

Heavy metal removal from sludge

In order to investigate the effect of substrate and plant types on the removal of Zn and Ni from sludge, cathode sludge samples

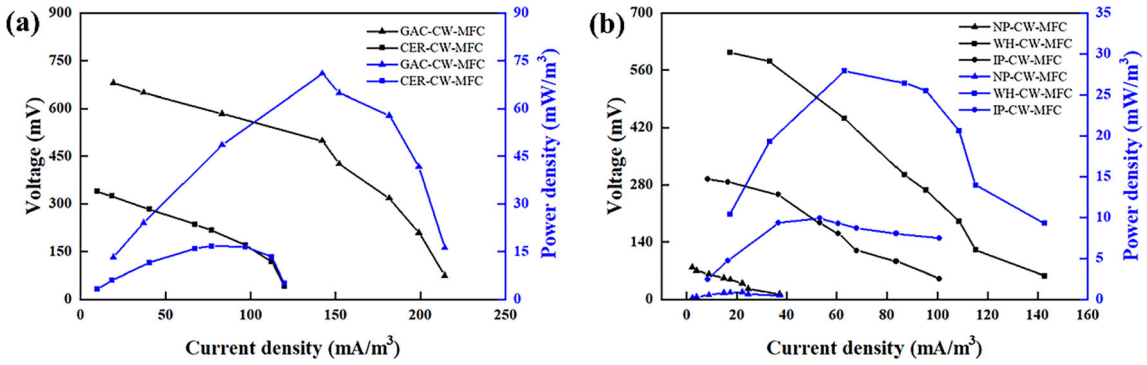

Fig. 3 Polarization curves of different substrates (**a**) and wetland plants (**b**)

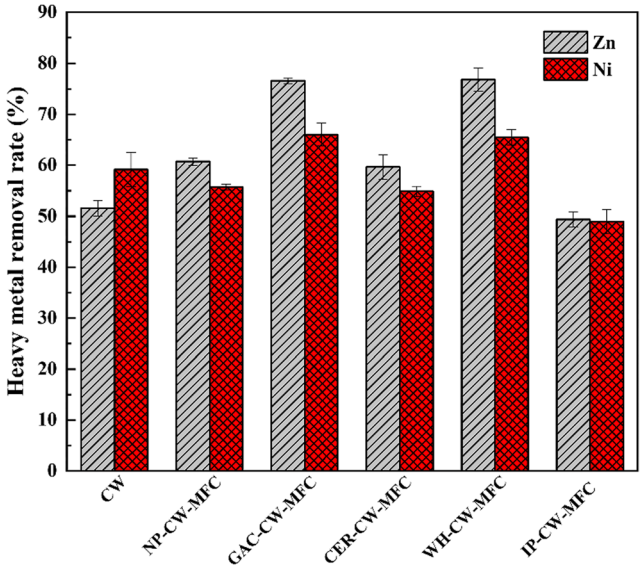

Fig. 4 Effect of different substrates and wetland plants on the removal of Zn and Ni from sludge. Data were shown as Mean±SE of 3 replicates

from six CW-MFC systems were collected after a 2-month operation period. As viewed in Fig. 4, almost more than 50% removal of Zn and Ni was obtained in six systems. GAC-CW-MFC produced the maximum Zn and Ni removal efficiencies of 76.88% and 66.02%, which were, respectively, about 25% and 7% higher than that of CW. On the one hand, the root exudates produced by plants were found to stimulate the activity and growth of rhizosphere microorganisms and wetland plants causing enhanced pollutant removal (Wang et al. 2017). On the other hand, organics were oxidized as electron donors by electrochemically active microorganisms at the anode to produce electrons and protons. Thereinto, the electrons were transferred to the anode surface by means of unique extracellular transport system and then conducted to the cathode via an external circuit to participate in the reduction and removal of high-valence heavy metals in the sludge (Gupta et al. 2021). Also, it had been reported that MFCs could remove heavy metals by the electrogenerated H_2O_2 at the cathode driven by iron-reducing bacteria (Liu et al. 2011). Thus, the integrated CW-MFC in closed circuit performed superior to that in open circuit (CW) with respect to Zn and Ni removal from sludge.

Upper Zn and Ni removal rates were achieved in GAC-CW-MFC device as compared to CER-CW-MFC, indicating that GAC enhanced heavy metal removal seriously. Carbonaceous materials, such as activated carbon and graphite granules, had been proven to possess the large specific surface area for the adhesion and growth of microbes (Fang et al. 2017). Meanwhile, its good electrical conductivity also contributed to facilitating the activity of cathode electrochemically active bacteria, thereby reducing the charge transfer resistance and accelerating the transfer of electrons from cathode to high-valence heavy metal ions to accomplish the effective removal (Zhang et al. 2019). In system NP-CW-MFC, 60.93% and 55.91% removal of Zn and Ni was obtained, respectively, which was lower than those in WH-CW-MFC but higher than those in IP-CW-MFC (seen in Fig. 4). It indicated that the heavy metal removal by CW-MFCs differed remarkably as a result of adding different types of wetland plants. Among these, *water hyacinth* displayed a positive effect due to its high absorption capacity of heavy metals and the catalysis on microbial metabolism (Saz et al. 2018). In addition, the corresponding system WH-CW-MFC with high output voltage enabled the transfer of electrons to the cathode at a faster speed, which increased the cathodic reaction rate (Rismani-Yazdi et al. 2011).

Migration and transformation of heavy metals

Migration of Zn and Ni

As shown in Table 3, the enrichment capacity of Zn and Ni in roots of each system was stronger than that in stems and

Table 3 The enrichment of heavy metals by plants in each system

Systems	Dry weight (g)		Heavy metal	Content ($mg \cdot kg^{-1}$)		Enrichment rate (%)	
	Roots	Stems and leaves		Roots	Stems and leaves	Roots	Stems and leaves
CW	0.2136	0.5274	Zn	750.00	364.00	9.26	4.49
			Ni	355.33	122.71	8.88	3.07
GAC-CW-MFC	0.2284	0.5457	Zn	1790.00	623.90	22.10	7.70
			Ni	579.28	204.50	14.48	5.11
CER-CW-MFC	0.2156	0.5198	Zn	871.00	243.62	10.75	3.01
			Ni	360.02	121.40	9.00	3.04
WH-CW-MFC	0.2398	0.5546	Zn	1709.50	615.32	21.10	7.60
			Ni	546.00	199.20	13.65	4.98
IP-CW-MFC	1.6207	1.7588	Zn	832.10	221.12	10.27	2.73
			Ni	390.40	142.44	9.76	3.56

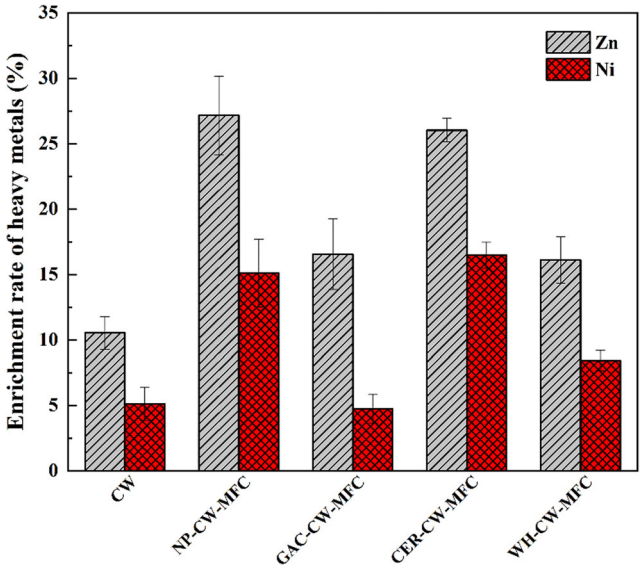

Fig. 5 The enrichment rates of heavy metals in each system cathode. Data were shown as Mean±SE of 3 replicates

leaves. It was speculated that most of the heavy metal elements could be absorbed by the plant roots immersed in the sludge, whereas needed to be transported to the stems and leaves. The enrichment rates of Zn and Ni reached 13.75% and 11.95% for CW, 29.8% and 19.59% for GAC-CW-MFC, and 13.76% and 12.04% for CER-CW-MFC, respectively. Obviously, the integration of a MFC could enhance the enrichment of Zn and Ni in CWs. Apparent differences in the enrichment of heavy metals in presence of different wetland plants were also noted. The plant biomass of GAC-CW-MFC was approximately 0.03 and 0.04 g higher than that of CW and CER-CW-MFC, respectively. On the one hand, microcurrent environment was beneficial to the growth of plants to some extent (Zhou et al. 2018). On the other hand, more biomass production in CW-MFCs could generate more bioelectricity and improve the aerobic microbial activity, thereby facilitating the pollutant removal (Di et al. 2020). Briefly, plant biomass and electrical performance were mutually reinforcing. The enrichment of heavy metals in system WH-CW-MFC was much higher than that in IP-CW-MFC, while the

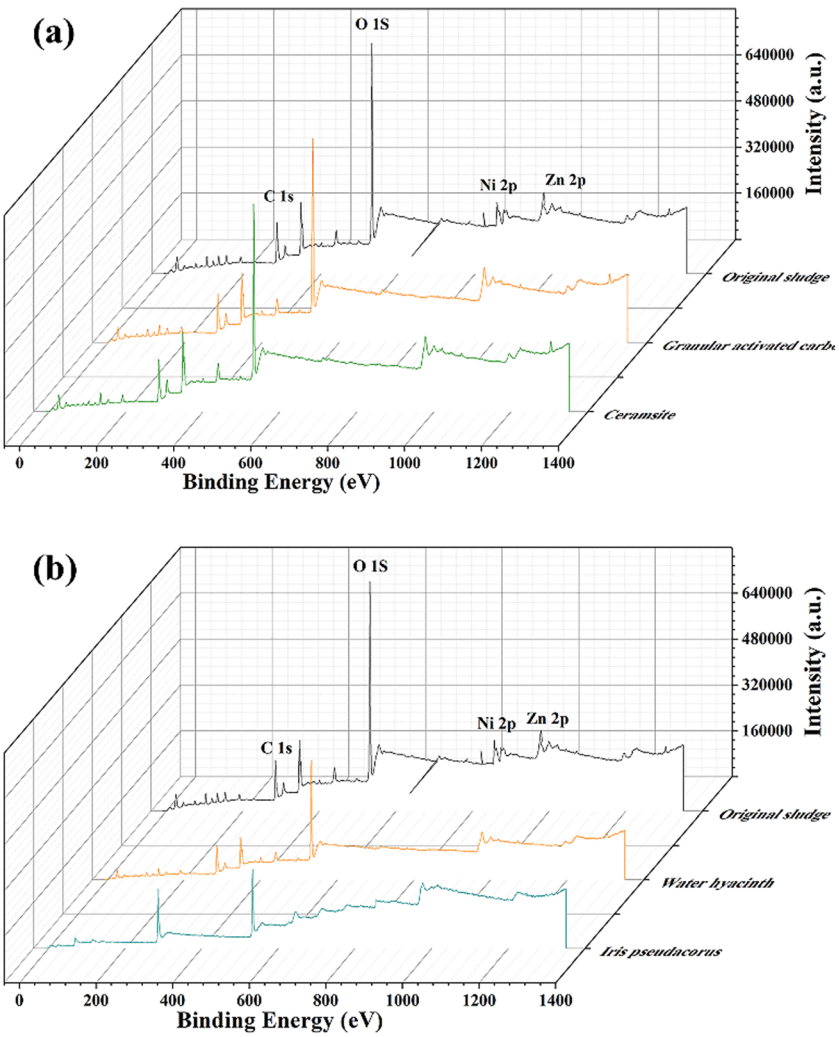

Fig. 6 XPS full spectrum of the original sludge and the sludge treated by different substrates (**a**) and plants (**b**)

biomass presented the opposite results. This abnormal phenomenon might be owing to the fact that *Iris pseudacorus* rooted beneath the sludge layer during the experiment, which greatly reduced its absorption and metabolism of Zn and Ni from sludge. Hence, the wetland plant *water hyacinth* with good anti-sludge performance could be considered as candidate against potential toxic effects of sludge.

Heavy metals (Zn and Ni) were enriched not only by the plants, but also near the cathode to achieve the removal. The enrichment properties of Zn and Ni for each system cathode

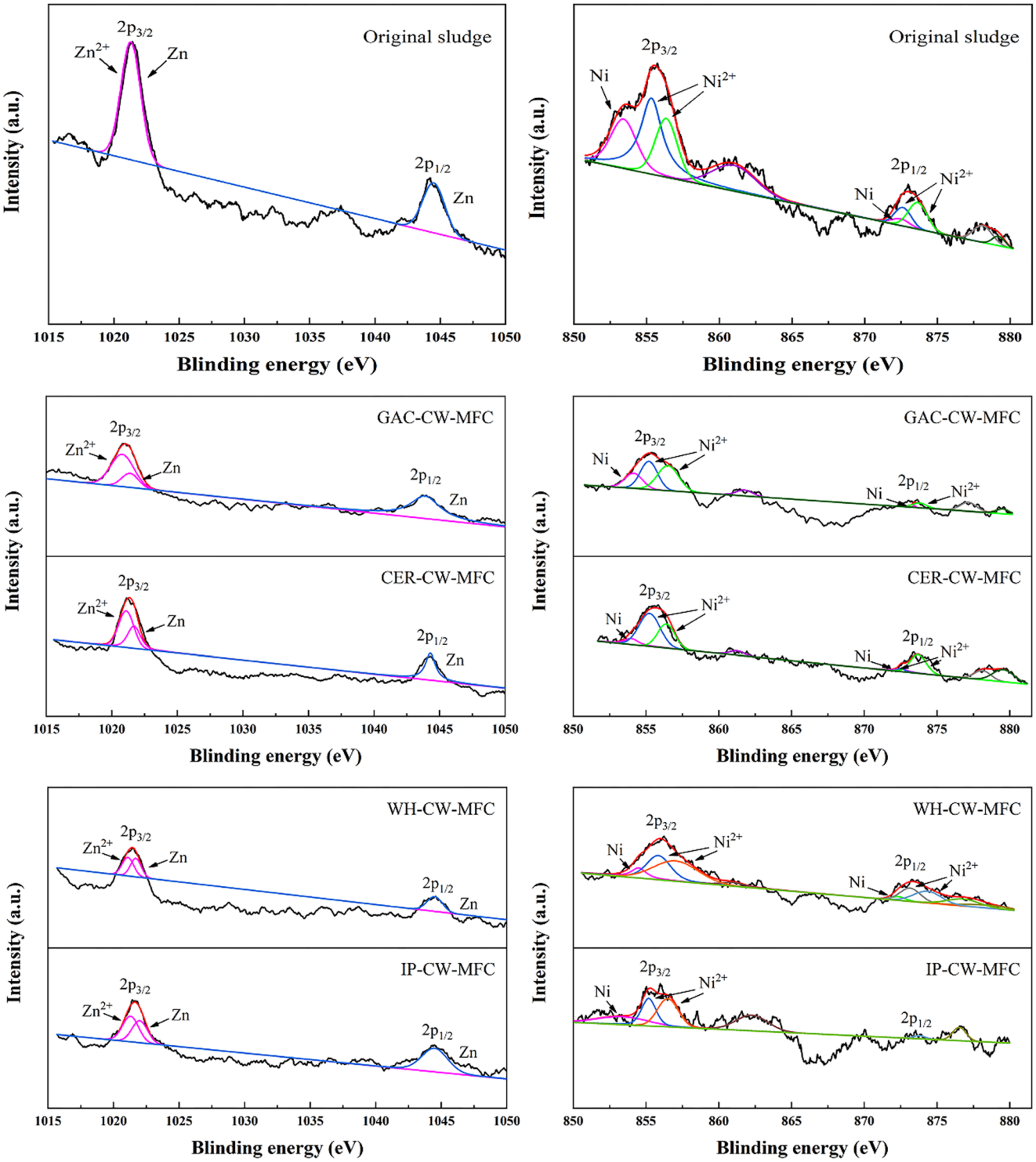

Fig. 7 Zn2p and Ni2p spectrograms of the original sludge and the sludge treated by different systems

were presented in Fig. 5. GAC-CW-MFC cathode showed the highest enrichment rates of Zn and Ni (27.16% and 15.13%, respectively) in comparison with NP-CW-MFC and CER-CW-MFC cathode. This confirmed that the heavy metal removal in CW-MFCs occurred more readily by GAC addition than by the ceramsite. Additionally, *water hyacinth* contributed more to the enrichment of Zn and Ni on the cathode as compared to *Iris pseudacorus*.

Chemical form transformation of Zn and Ni

As presented in Fig. 6, the main peaks observed at 285 and 531 eV corresponded to the C1s and O1s bands, respectively. Simultaneously, the addition peaks detectable at 853 and 1022 eV were attributed to Ni 2p and Zn 2p. C1s was caused by exposure to the small molecules in CO_2, air, and water. The high peak position (531 eV) of O1s was attributed to the high oxygen content of sludge at the system cathode and classified as the peak of chemisorbed oxygen on the surface (Ahmed et al. 2013).

Zn2p and Ni2p spectrograms of the sludge treated by different substrates and plants were displayed in Fig. 7. The Zn 2p3/2 peaks were relatively sharp and exhibited at binding energy characteristic (i.e., 1021.3 eV and 1021.7 eV) of Zn and Zn^{2+} (Blumentrit et al. 2011; Wu et al. 2017). The binding energy of Zn 2p1/2 was located at 1045.0 eV. These results indicated that Zn mainly combined with oxygen in the form of Zn^{2+}, namely ZnO (Morozov et al. 2015). Six separated peaks at 853.4, 855.3, 856.342, 872.4, 872.6, and 873.6 eV were observed for metallic Ni (2p3/2), NiO (2p3/2), $Ni(OH)_2$ (2p3/2), metallic Ni (2p1/2), NiO (2p1/2), and $Ni(OH)_2$ (2p1/2), respectively (Pattanayak et al. 2019; Vivet et al. 2020). After a 60-day operation period, the satellite peaks of Zn2p and Ni2p became smaller, especially in systems GAC-CW-MFC and WH-CW-MFC, indicating that the high-valence Zn and Ni were continuously reduced to low-valence or elemental substances (Liu et al. 2015).

The peak positions of Zn2p and Ni2p had scarcely any displacement during the operation. The binding energies of Zn2p and Ni2p shifted slightly to the direction of higher ones accompanied by optimizing the substrate and plant types. The Zn and Ni contents on the sludge surface decreased due to their formation of metal oxides (Sheng et al. 2011). In summary, the obtained XPS results would provide evidences in proving the reduction and removal of metal ions on the cathode by gaining the electronics (Liu et al. 2019).

Conclusions

The impacts of different substrates and plants towards the heavy metal (Zn and Ni) treatment of sludge as well as electricity generation in CW-MFCs were evaluated. Among these, GAC and *water hyacinth* was, respectively, the most effective promoter. The corresponding CW-MFCs produced the maximum Zn and Ni removal efficiencies of 76.88% and 66.02%, which induced, respectively, about 25% and 7% improvement in comparison with CW. Meanwhile, GAC- and WH-CW-MFC displayed remarkable superiority with respect to enhancing ORP gradient, output voltage, and power density. Plant roots and electrodes were confirmed to play major roles in the migration of Zn and Ni. The main heavy metals on the sludge surface were analyzed as Zn and Ni. Besides, the high-valence Zn and Ni were effectively reduced to low-valence or elemental metals. Our findings provide a theoretical guidance for the resource utilization of municipal sludge. Furthermore, the CW-MFC signifies its potential application prospects in the removal of heavy metals from sludge.

Author contribution DX formulated overarching research goals and aims. LW and TL performed material preparation, data collection, and analysis. The first draft of the manuscript was written by LW. Revision was charged by QZ and ZT. All authors commented on previous versions of the manuscript. All authors read and approved the final manuscript.

Funding This study was supported by the Key Research and Development Program of Anhui Provincial Science Technology Department (201904a07020083), the Key Program of Anhui Polytechnic University (Xjky2020086), and the Anhui Polytechnic University "Young and Middle-Aged Top Talent" Training Program.

Data availability Not applicable.

Declarations

Ethics approval and consent to participate Not applicable.

Consent for publication Not applicable.

Competing interests The authors declare no competing interests.

References

Ahmed MH, Byrne JA, McLaughlin J, Ahmed W (2013) Study of human serum albumin adsorption and conformational change on DLC and silicon doped DLC using XPS and FTIR spectroscopy. J Biomater Nanobiotechnol 04(02):194–203. https://doi.org/10.4236/jbnb.2013.42024

Blumentrit P, Yoshitake M, Nemšák S, Kim T, Nagata T (2011) XPS and UPS study on band alignment at Pt–Zn-terminated ZnO(0001) interface. Appl Surf Sci 258(2):780–785. https://doi.org/10.1016/j.apsusc.2011.08.095

Chen SY, Cheng YK (2019) Effects of sulfur dosage and inoculum size on pilot-scale thermophilic bioleaching of heavy metals from sewage sludge. Chemosphere 234:346–355. https://doi.org/10.1016/j.chemosphere.2019.06.084

Chen Z, Huang YC, Liang JH, Zhao F, Zhu YG (2012) A novel sediment microbial fuel cell with a biocathode in the rice rhizosphere.

Bioresour Technol 108:55–59. https://doi.org/10.1016/j.biortech.2011.10.040

Di L, Li Y, Nie L, Wang S, Kong F (2020) Influence of plant radial oxygen loss in constructed wetland combined with microbial fuel cell on nitrobenzene removal from aqueous solution. J Hazard Mater 394:122542. https://doi.org/10.1016/j.jhazmat.2020.122542

Doherty L, Zhao Y, Zhao X, Hu Y, Hao X, Xu L, Liu R (2015) A review of a recently emerged technology: constructed wetland–microbial fuel cells. Water Res 85:38–45. https://doi.org/10.1016/j.watres.2015.08.016

Fan J, Zhang B, Zhang J, Ngo HH, Guo W, Liu F, Guo Y, Wu H (2013) Intermittent aeration strategy to enhance organics and nitrogen removal in subsurface flow constructed wetlands. Bioresour Technol 141:117–122. https://doi.org/10.1016/j.biortech.2013.03.077

Fang Z, Song HL, Cang N, Li XN (2013) Performance of microbial fuel cell coupled constructed wetland system for decolorization of azo dye and bioelectricity generation. Bioresour Technol 144:165–171. https://doi.org/10.1016/j.biortech.2013.06.073

Fang Z, Cheng S, Wang H, Cao X, Li X (2017) Feasibility study of simultaneous azo dye decolorization and bioelectricity generation by microbial fuel cell-coupled constructed wetland: substrate effects. RSC Adv 7(27):16542–16552. https://doi.org/10.1039/c7ra01255a

Gao J, Luo Q, Zhang C, Li B, Meng L (2013) Enhanced electrokinetic removal of cadmium from sludge using a coupled catholyte circulation system with multilayer of anion exchange resin. Chem Eng J 234:1–8. https://doi.org/10.1016/j.cej.2013.08.019

Ge X, Cao X, Song X, Wang Y, Si Z, Zhao Y, Wang W, Tesfahunegn AA (2020) Bioenergy generation and simultaneous nitrate and phosphorus removal in a pyrite-based constructed wetland-microbial fuel cell. Bioresour Technol 296:122350. https://doi.org/10.1016/j.biortech.2019.122350

Gupta S, Srivastava P, Patil SA, Yadav AK (2021) A comprehensive review on emerging constructed wetland coupled microbial fuel cell technology: potential applications and challenges. Bioresour Technol 320(Pt B):124376. https://doi.org/10.1016/j.biortech.2020.124376

Helder M, Strik DP, Hamelers HV, Kuhn AJ, Blok C, Buisman CJ (2010) Concurrent bio-electricity and biomass production in three plant-microbial fuel cells using Spartina anglica, Arundinella anomala and Arundo donax. Bioresour Technol 101(10):3541–3547. https://doi.org/10.1016/j.biortech.2009.12.124

Hu S, Hu J, Sun Y, Zhu Q, Wu L, Liu B, Xiao K, Liang S, Yang J, Hou H (2021) Simultaneous heavy metal removal and sludge deep dewatering with Fe(II) assisted electrooxidation technology. J Hazard Mater 405:124072. https://doi.org/10.1016/j.jhazmat.2020.124072

Ke X, Zhang G, Wan T, Gao F (2012) Heavy-metal accumulation in low-sludge wastewater treatment technique: sonication-cryptic growth. J Environ Eng 138(3):248–251. https://doi.org/10.1061/(asce)ee.1943-7870.0000418

Li M, Zhou S, Xu Y, Liu Z, Ma F, Zhi L, Zhou X (2018) Simultaneous Cr(VI) reduction and bioelectricity generation in a dual chamber microbial fuel cell. Chem Eng J 334:1621–1629. https://doi.org/10.1016/j.cej.2017.11.144

Liu L, Yuan Y, Li FB, Feng CH (2011) In-situ Cr(VI) reduction with electrogenerated hydrogen peroxide driven by iron-reducing bacteria. Bioresour Technol 102(3):2468–2473. https://doi.org/10.1016/j.biortech.2010.11.013

Liu S, Song H, Wei S, Yang F, Li X (2014) Bio-cathode materials evaluation and configuration optimization for power output of vertical subsurface flow constructed wetland - microbial fuel cell systems. Bioresour Technol 166:575–583. https://doi.org/10.1016/j.biortech.2014.05.104

Liu W, Zhang J, Jin Y, Zhao X, Cai Z (2015) Adsorption of Pb(II), Cd(II) and Zn(II) by extracellular polymeric substances extracted from aerobic granular sludge: efficiency of protein. J Environ Chem Eng 3(2):1223–1232. https://doi.org/10.1016/j.jece.2015.04.009

Liu B, Ji M, Zhai H (2018a) Anodic potentials, electricity generation and bacterial community as affected by plant roots in sediment microbial fuel cell: effects of anode locations. Chemosphere 209:739–747. https://doi.org/10.1016/j.chemosphere.2018.06.122

Liu T, Liu Z, Zheng Q, Lang Q, Xia Y, Peng N, Gai C (2018b) Effect of hydrothermal carbonization on migration and environmental risk of heavy metals in sewage sludge during pyrolysis. Bioresour Technol 247:282–290. https://doi.org/10.1016/j.biortech.2017.09.090

Liu W, Zheng J, Ou X, Liu X, Song Y, Tian C, Rong W, Shi Z, Dang Z, Lin Z (2018c) Effective extraction of Cr(VI) from hazardous gypsum sludge via controlling the phase transformation and chromium species. Environ Sci Technol 52(22):13336–13342. https://doi.org/10.1021/acs.est.8b02213

Liu Y, Song P, Gai R, Yan C, Jiao Y, Yin D, Cai L, Zhang L (2019) Recovering platinum from wastewater by charring biofilm of microbial fuel cells (MFCs). J Saudi Chem Soc 23(3):338–345. https://doi.org/10.1016/j.jscs.2018.08.003

Liu T, Xu D, Wang L, Yang W, Xia Y (2020) Effect of electrode spacing on the removal of Zn and Ni in sludge and its electricity generation performance by CW-MFC. Chem Ind Eng Prog 1–13 (in Chinese). https://doi.org/10.16085/j.issn.1000-6613.2020-1665

Logan BE, Hamelers B, Rozendal R, Schröder U, Keller J, Freguia S, Aelterman P, Verstraete W, Rabaey K (2006) Microbial fuel cells: methodology and technology. Environ Sci Technol 40(17):5181–5192. https://doi.org/10.1021/es0605016

Meng D, Wu J, Xu Z, Xu Y, Li H, Jin W, Zhang J (2020) Effect of passive ventilation on the performance of unplanted sludge treatment wetlands: heavy metal removal and microbial community variation. Environ Sci Pollut Res Int 27(25):31665–31676. https://doi.org/10.1007/s11356-020-09288-w

Morozov IG, Belousova OV, Ortega D, Mafina MK, Kuznetcov MV (2015) Structural, optical, XPS and magnetic properties of Zn particles capped by ZnO nanoparticles. J Alloys Compd 633:237–245. https://doi.org/10.1016/j.jallcom.2015.01.285

Mu C, Wang L, Wang L (2020) Performance of lab-scale microbial fuel cell coupled with unplanted constructed wetland for hexavalent chromium removal and electricity production. Environ Sci Pollut Res Int 27(20):25140–25148. https://doi.org/10.1007/s11356-020-08982-z

Pattanayak P, Papiya F, Kumar V, Pramanik N, Kundu PP (2019) Deposition of Ni–NiO nanoparticles on the reduced graphene oxide filled polypyrrole: evaluation as cathode catalyst in microbial fuel cells. Sustain Energy Fuels 3(7):1808–1826. https://doi.org/10.1039/c9se00055k

Qian L, Wang S, Xu D, Guo Y, Tang X, Wang L (2016) Treatment of municipal sewage sludge in supercritical water: a review. Water Res 89:118–131. https://doi.org/10.1016/j.watres.2015.11.047

Rismani-Yazdi H, Christy AD, Carver SM, Yu Z, Dehority BA, Tuovinen OH (2011) Effect of external resistance on bacterial diversity and metabolism in cellulose-fed microbial fuel cells. Bioresour Technol 102(1):278–283. https://doi.org/10.1016/j.biortech.2010.05.012

Saz C, Ture C, Turker OC, Yakar A (2018) Effect of vegetation type on treatment performance and bioelectric production of constructed wetland modules combined with microbial fuel cell (CW-MFC) treating synthetic wastewater. Environ Sci Pollut Res Int 25(9):8777–8792. https://doi.org/10.1007/s11356-018-1208-y

Shamsollahi HR, Alimohammadi M, Momeni S, Naddafi K, Nabizadeh R, Khorasgani FC, Masinaei M, Yousefi M (2019) Assessment of the health risk induced by accumulated heavy metals from anaerobic digestion of biological sludge of the lettuce. Biol Trace Elem Res 188(2):514–520. https://doi.org/10.1007/s12011-018-1422-y

Shen X, Zhang J, Liu D, Hu Z, Liu H (2018) Enhance performance of microbial fuel cell coupled surface flow constructed wetland by

using submerged plants and enclosed anodes. Chem Eng J 351:312–318. https://doi.org/10.1016/j.cej.2018.06.117

Sheng G, Yang S, Sheng J, Hu J, Tan X, Wang X (2011) Macroscopic and microscopic investigation of Ni(II) sequestration on diatomite by batch, XPS, and EXAFS techniques. Environ Sci Technol 45(18):7718–7726. https://doi.org/10.1021/es202108q

Srivastava P, Yadav AK, Mishra BK (2015) The effects of microbial fuel cell integration into constructed wetland on the performance of constructed wetland. Bioresour Technol 195:223–230. https://doi.org/10.1016/j.biortech.2015.05.072

Srivastava P, Dwivedi S, Kumar N, Abbassi R, Garaniya V, Yadav AK (2017) Performance assessment of aeration and radial oxygen loss assisted cathode based integrated constructed wetland-microbial fuel cell systems. Bioresour Technol 244(Pt 1):1178–1182. https://doi.org/10.1016/j.biortech.2017.08.026

Teoh T-P, Ong S-A, Ho L-N, Wong Y-S, Oon Y-L, Oon Y-S, Tan S-M, Thung W-E (2020) Up-flow constructed wetland-microbial fuel cell: Influence of floating plant, aeration and circuit connection on wastewater treatment performance and bioelectricity generation. J Water Process Eng 36:101371. https://doi.org/10.1016/j.jwpe.2020.101371

Villasenor J, Capilla P, Rodrigo MA, Canizares P, Fernandez FJ (2013) Operation of a horizontal subsurface flow constructed wetland–microbial fuel cell treating wastewater under different organic loading rates. Water Res 47(17):6731–6738. https://doi.org/10.1016/j.watres.2013.09.005

Vivet L, Benoit R, Falzon MF, Tan KL, Dorairaj D, Morelle JM (2020) XPS, ToF SIMS and wettability analyses on Ni surfaces after Ar-H2 RF plasma treatment: an efficient and optimized plasma treatment approach. Surf Coat Technol 398:126094. https://doi.org/10.1016/j.surfcoat.2020.126094

Wang J, Song X, Wang Y, Bai J, Bai H, Yan D, Cao Y, Li Y, Yu Z, Dong G (2017) Bioelectricity generation, contaminant removal and bacterial community distribution as affected by substrate material size and aquatic macrophyte in constructed wetland-microbial fuel cell. Bioresour Technol 245(Pt A):372–378. https://doi.org/10.1016/j.biortech.2017.08.191

Wang X, Tian Y, Liu H, Zhao X, Wu Q (2019) Effects of influent COD/TN ratio on nitrogen removal in integrated constructed wetland-microbial fuel cell systems. Bioresour Technol 271:492–495. https://doi.org/10.1016/j.biortech.2018.09.039

Wang Y, Cai Z, Sheng S, Pan F, Chen F, Fu J (2020) Comprehensive evaluation of substrate materials for contaminants removal in constructed wetlands. Sci Total Environ 701:134736. https://doi.org/10.1016/j.scitotenv.2019.134736

Wu Z-W, Tyan S-L, Chen H-H, Huang J-C-A, Huang Y-C, Lee C-R, Mo T-S (2017) Temperature-dependent photoluminescence and XPS study of ZnO nanowires grown on flexible Zn foil via thermal oxidation. Superlattice Microst 107:38–43. https://doi.org/10.1016/j.spmi.2017.04.016

Xu F, Ouyang DL, Rene ER, Ng HY, Guo LL, Zhu YJ, Zhou LL, Yuan Q, Miao MS, Wang Q, Kong Q (2019) Electricity production enhancement in a constructed wetland-microbial fuel cell system for treating saline wastewater. Bioresour Technol 288:121462. https://doi.org/10.1016/j.biortech.2019.121462

Xu H, Song HL, Singh RP, Yang YL, Xu JY, Yang XL (2021) Simultaneous reduction of antibiotics leakage and methane emission from constructed wetland by integrating microbial fuel cell. Bioresour Technol 320(Pt A):124285. https://doi.org/10.1016/j.biortech.2020.124285

Yang J, Zhao C, Xing M, Lin Y (2013) Enhancement stabilization of heavy metals (Zn, Pb, Cr and Cu) during vermifiltration of liquid-state sludge. Bioresour Technol 146:649–655. https://doi.org/10.1016/j.biortech.2013.07.144

Zhang J, Zhou X, Wang H, Zhu D, Li X (2019) Research advances in treatment of heavy metal wastewater by microbial fuel cells. CIESC J 70(06):2027–2035 (in Chinese). https://doi.org/10.11949/j.issn.0438-1157.20181308

Zhang K, Wu X, Luo H, Li X, Chen W, Chen J, Mo Y, Wang W (2020) CH_4 control and associated microbial process from constructed wetland (CW) by microbial fuel cells (MFC). J Environ Manag 260:110071. https://doi.org/10.1016/j.jenvman.2020.110071

Zhao C, Shang D, Zou Y, Du Y, Wang Q, Xu F, Ren L, Kong Q (2020) Changes in electricity production and microbial community evolution in constructed wetland-microbial fuel cell exposed to wastewater containing Pb(II). Sci Total Environ 732:139127. https://doi.org/10.1016/j.scitotenv.2020.139127

Zhong F, Yu C, Chen Y, Wu X, Wu J, Liu G, Zhang J, Deng Z, Cheng S (2020) Nutrient removal process and cathodic microbial community composition in integrated vertical-flow constructed wetland - microbial fuel cells filled with different substrates. Front Microbiol 11:1896. https://doi.org/10.3389/fmicb.2020.01896

Zhou Y, Xu D, Xiao E, Xu D, Xu P, Zhang X, Zhou Q, He F, Wu Z (2018) Relationship between electrogenic performance and physiological change of four wetland plants in constructed wetland-microbial fuel cells during non-growing seasons. J Environ Sci (China) 70:54–62. https://doi.org/10.1016/j.jes.2017.11.008

Zhou G, Gu Y, Yuan H, Gong Y, Wu Y (2020) Selecting sustainable technologies for disposal of municipal sewage sludge using a multi-criterion decision-making method: a case study from China. Resour Conserv Recycl 161:104881. https://doi.org/10.1016/j.resconrec.2020.104881